Medium-range structural order in covalent amorphous solids

S. R. Elliott

Despite their lack of long-range translational and orientational order, covalent amorphous solids can exhibit structural order over both short and medium length scales, the latter reaching to 20 Å or so. Medium-range order is difficult to measure experimentally and to interpret unambiguously, but a variety of techniques have allowed several types of characteristic structural ordering to be identified and their origin elucidated.

HOW disordered is the atomic structure of an amorphous solid? Although it is indisputable that such structures are devoid of long-range translational periodicity, the question of the degree of residual structural order present in a noncrystalline material at shorter length scales remains controversial.

Disorder in materials can be manifested in many ways: examples are vibrational, spin and orientational disorder (all referred to a periodic lattice) and topological disorder. I will concentrate principally on the latter, which is the type of disorder associated with the structure of glassy and amorphous solids in which the structure cannot be defined in terms of a periodic lattice.

Determination of the atomic structure of amorphous materials is unfortunately a non-trivial task. Because the structure can be defined essentially only in terms of a 'unit cell' containing an infinitely large number of atoms (as there is no long-range periodic symmetry), a statistical description is unavoidable. The structure of a particular amorphous solid can therefore never be determined unambiguously, and this uncertainty is compounded by the fact that the structure of a noncrystalline material, at both microscopic and macroscopic levels, often depends on details of the method of preparation. Furthermore, in general, more than one experimental structural probe must be used to obtain as full a picture as possible of the structural arrangement in an amorphous solid (see Box 1).

In discussing the structure of amorphous materials, it is useful to consider the types of structural order that can exist in such materials at various length scales. Such a categorization is convenient in two regards: the classification is hierarchical, so that a particular type of order at one length scale can be dictated by order at a smaller scale (but not necessarily the converse); and the various experimental probes are generally sensitive to structural correlations at different length scales. For reasons of definiteness and brevity, I will consider only covalently bonded amorphous solids, for it is in these materials that the degree and extent of medium-range order is maximized because of the stereochemical (directed) bonding.

Classification of structural order

We can consider three contiguous length scales[1]: short-range order (SRO) in the range 2–5 Å; medium-range order (MRO) in the range 5–20 Å; and long-range structure (LRS) at distances $\geq$20 Å (by definition there is no long-range *order*, in the form of translational periodicity, in the structure of a glass).

In the case of covalent materials, where directed bonding is dominant, SRO can be characterized in terms of well-defined coordination polyhedra (see Fig. 1*a*). The parameters needed to describe topological SRO are the number, N_j of nearest neighbours, j, around an origin atom of type i, the nearest-neighbour bond-length R_{ij}, the bond angle θ_{jik} subtended at atom i (where atom type k may be different from j), and the corresponding quantities when atom j is regarded as the origin, thereby defining the connectivity of the polyhedra.

In addition, the chemical SRO needs to be considered when different types of atoms constitute the coordination polyhedron centred on a particular atom. For nonstoichiometric compositions, excess atoms are accommodated by the formation of 'wrong' (for example, homopolar) bonds, in the absence of coordination or valence changes, and the chemical order that might otherwise occur at the stoichiometric composition is thereby broken; the relevant parameter here is then the fraction of wrong bonds per coordination polyhedron. (Mössbauer

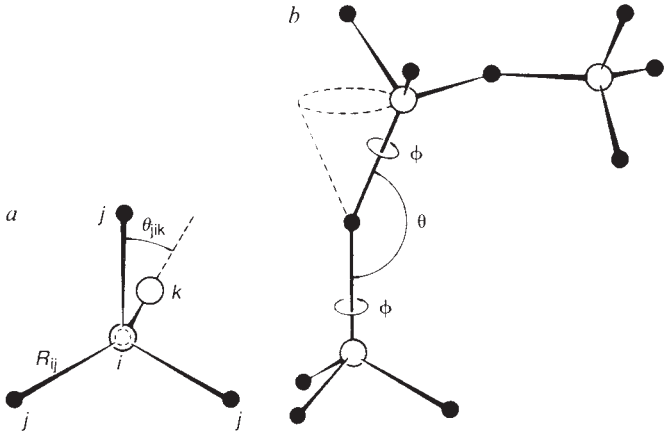

FIG. 1 Illustrations of short-range order (SRO) and medium-range order (MRO). *a*, SRO defined in terms of coordination polyhedra (two- and three-body correlations). *b*, Near MRO defined in terms of connection of polyhedra. The definition of the dihedral angle (ϕ) is shown (four-body correlation).

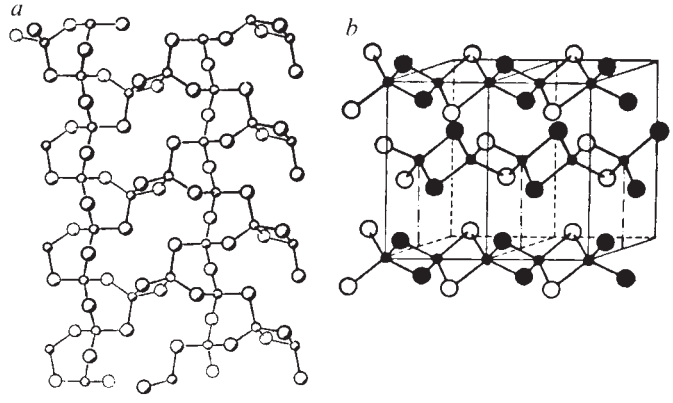

FIG. 2 Structures of crystalline GeX_2 and SiX_2 materials (X is S, Se). *a*, $GeS_2/GeSe_2$, showing 25% proportion of edge-shared tetrahedra resulting in a sheet-like structure. *b*, $SiS_2/SiSe_2$, showing 100% edge-shared tetrahedra, resulting in a chain-like structure.

spectroscopy can be sensitive to such broken chemical order in certain circumstances[2].) A related situation is when the different atomic species in the coordination shell around a given origin atom are in fact the same element, but each ligand can have a different charge state, bonding connectivity and so on. An example is the case of 'non-bridging oxygen' atoms (singly bonded, singly negatively charged) introduced into oxide glasses by the incorporation of alkali modifier atoms; for silicates, such configurations are denoted as Q_n ('quaternary') species, where n (=0-4) is the number of bridging (doubly coordinated) oxygens in the coordination polyhedron (tetrahedron) centred on a silicon atom.

The definition of MRO is more contentious[1,3-5], but it can simply be regarded as the next highest level of structural organization beyond SRO. In practice, it is helpful to subdivide the types of MRO into three categories[1], corresponding to increasing length scales. At the shortest length scale (say ≤ 5 Å), near-MRO (NMRO) describes the type of connection between the coordination polyhedra. Thus, corner-, edge- or face-sharing of polyhedra leads to very different ordering arrangements on a local scale. A parameter that can be used as a description of the orientational correlations associated with such connectivity is the 'dihedral' (or torsion) angle, ϕ, defined as the angle of rotation about a common bond required to bring into coincidence the projections, on the plane perpendicular to this bond, of the other bonds in the connected units (see Fig. 1*b*). Thus, NMRO is characterized by four-body correlations. Departures from a uniform (that is, random) distribution of ϕ are correspondingly a hallmark of MRO.

At the next length scale (say ~5-8 Å), intermediate MRO (IMRO) can be associated with correlations (phase relationships) between pairs of preferred dihedral angles for neighbouring bonds—that is, triplet correlations between connected polyhedra or, in other words, five-body correlations. Thus, a pronounced degree of IMRO is associated with coordination polyhedra connected together in well-defined relative orientations. This circumstance leads naturally to the occurrence of 'superstructural' units[1], which are aggregates of basic polyhedra connected together to form regular rings, or three-dimensional clusters (see Fig. 1*c*), which can be regarded as constituting alternative building blocks of the structure if they exist in a significantly higher proportion than would be expected on a random statistical basis.

Finally, on a yet larger length scale (say 8-20 Å), far-MRO (FMRO) can be associated with the local dimensionality of the covalently bonded amorphous network; this can be ascertained by finding the dimension traced out locally (over distances ≤ 20 Å) by a process of bond percolation among the covalent bonds of the structure, neglecting the much weaker Van der Waals bonds[6]. A local dimensionality of 3 would correspond to structural isotropy; local dimensionalities of 2 (layer-like), 1 (chain-like) or 0 (isolated cluster) can arise either from the type of connection between structural units (for example, one-dimensional chain-like structures resulting from edge-sharing of tetrahedra) or from network depolymerization associated with the formation of non-bridging ligands caused by the introduction of network-modifying cations into the structure.

Finally, at the largest length scale, LRS is associated with inhomogeneities in the structure, such as voids and columnar growth morphology in films. Here I will not discuss such large-scale structural imperfections further, concentrating instead on medium-range order.

Polyhedral connections

Appreciable variations in the type of connections between coordination polyhedra are found in the good glass-forming system, AX_2 (A is Si or Ge; X is O, S or Se), where the coordination polyhedra are AX_4 tetrahedra[1]. For the oxides, SiO_2 and GeO_2, connection is by corner-sharing of tetrahedra through the O atoms; this results in the formation of three-dimensional structures with (relatively) little MRO. But the structures of the chemically analogous glasses, germanium and

BOX 1 Experimental structural probes

Several experimental techniques may be used to investigate the structure of amorphous solids, and specifically the MRO. Neutron (or X-ray) diffraction is the obvious choice, but it suffers from the disadvantage that for peaks other than the first (and perhaps the second) in the real-space radial distribution function, obtained by Fourier transformation of the scattering data, unambiguous interpretation in terms of n-neighbour correlations is not possible because of the overlap of higher-order peaks[1]. This problem is exacerbated for materials containing more than a single type of atom, if just one diffraction experiment is performed, as 'partial' structural information (the structural environment around a particular type of atom) cannot then be obtained. It may be possible to obtain partial structural information by using isotope substitution, if suitable isotopes exist with sufficiently different neutron scattering lengths, or anomalous scattering, if the X-ray photon energy can be tuned to lie either side of an X-ray absorption edge. In fact, diffraction data can only really provide information relating to MRO if it is compared with the calculated scattering characteristics of a structural model for which the atomic positions, and hence the MRO, are known. Nevertheless, the 'first sharp diffraction peak' observed in the structure factor has been regarded as a signature of MRO; a discussion of the structural origin of this peak is given in Box 2.

Other techniques can provide complementary information on MRO in glasses. These techniques should ideally be atom-specific, so that the structural environment of a particular type of atom can be probed, and they should also be sensitive to local conformation, that is, they should probe three-body (or higher) correlations, instead of the two-body correlations probed by conventional single-scattering diffraction experiments. One such method is nuclear magnetic resonance, which, when coupled with the use of 'magic-angle spinning' to reduce the effect of spectral broadening interactions operative in the solid state, can produce high-resolution spectra[1]. The method has the drawback that relatively few nuclei are suitable for study by NMR, and site disorder can cause such a degree of inhomogeneous broadening of resonance lines that a structural interpretation becomes impossible. Nevertheless, magic-angle spinning NMR is a powerful probe of certain aspects of MRO, such as clusters, where the degree of local order is such that structurally inequivalent sites can be distinguished because their resonance lines have resolvably different chemical shifts. Although most NMR spectra are interpreted by 'finger-printing', where the spectrum of the amorphous solid is compared with those of known, related structures (for example, spectra of molecular species in crystals or solution) to ascertain whether particular structural moieties are present, nevertheless quantitative (pair correlation) structural information can be obtained in principle from NMR experiments by making use of internuclear dipolar interactions whose strength varies as r^{-3}, where r is the interatomic spacing.

Vibrational spectroscopy, and in particular Raman scattering, is another non-diffraction structural probe which can be especially sensitive to the presence of MRO. Highly ordered regions of an amorphous structure, associated with a considerable degree of MRO, can support vibrational excitations which, when 'vibrationally decoupled' from the rest of the network, may produce intense, narrow Raman lines. Such signatures of MRO can be even more apparent if the vibrational mode of a superstructural unit is a symmetric breathing motion, as this will result in the associated Raman line being strongly polarized, (that is, the band measured in the HH configuration is considerably more intense than that measured in the HV configuration, where HH and HV refer to the polarization directions in the incident and scattered beams (H, horizontal; V, vertical)). Such symmetric modes can also lead to an enhanced matrix element for scattering; that is, stronger coupling constants relating the induced polarizability and the displacement amplitudes. As a result, Raman scattering is an extremely sensitive probe for the existence of regular superstructural units in the structure of amorphous solids, but, correspondingly, it is not a quantitative technique: the intensities of peaks in the HH Raman spectrum associated with MRO are generally greatly enhanced with respect to the integrated area of the corresponding feature in the true vibrational density of states.

silicon chalcogenides, seem to be intriguingly different. The low-pressure/low-temperature crystalline form of GeS_2 and $GeSe_2$ consists of 50% of the tetrahedra with edge-shared connections; these act as bridges for chains of corner-shared tetrahedra, thereby resulting in a sheet-like two-dimensional structure (Fig. 2*a*). In the low-pressure/low-temperature polymorph of crystalline SiS_2 and $SiSe_2$, all tetrahedra have edge-shared connections; this configuration results in a chain-like one-dimensional structure (Fig. 2*b*). There has been considerable controversy over the structures of glasses of these materials. Of particular concern is the extent of the similarity between crystalline and non-crystalline structures, as indicated by the proportion of edge-shared tetrahedra (that is, the NMRO[7,8]).

In the case of g-$GeSe_2$, high-resolution neutron diffraction[9] has provided clear evidence for anomalously short Ge–Ge distances in the structure, associated with the four-membered (Ge_2Se_2) rings characteristic of edge-shared connections between tetrahedral units (see Fig. 2). The fraction of edge-sharing tetrahedra found in the glass structure was ~40% (as compared with 50% for the crystal); a molecular-dynamics simulation[10] of the structure of g-$GeSe_2$, using three-body interaction potentials to mimic covalent forces, predicts ~32% edge-sharing tetrahedra, with a radial distribution function and structure factor in generally good agreement with the neutron data[9].

Neutron diffraction data also exist for g-$SiSe_2$ (refs 11, 12), and a systematic modelling study of the structure of this material, using serial addition of atoms, has been made in an attempt to fit the scattering data[13,14]. As in the structure of the crystalline polymorph, the dominant structural motif in the glass is found to be the edge-shared tetrahedron. The configuration of SiX_4 tetrahedra can be represented as E_n species, where E stands for edge-sharing, and n (=0–2) is the number of edge-shared connections per tetrahedral unit. Modelling studies[13,14] found, however, that not all tetrahedra had E_2 configurations; this implies that the structure of the glass is not composed entirely of random chains of linked tetrahedra, as originally suggested on the basis of a comparison of the Raman scattering data for the glass with that for the crystal[15,16]. A later interpretation[17] of the Raman spectra of g-Si_xSe_{1-x} led to the suggestion that some E_1 and E_0 tetrahedral configurations were also present. Further confirmation for the simultaneous presence of E_2, E_1 and E_0 configurations in the structure of SiX_2 glasses (where X is S, Se) has come from ^{29}Si magic-angle-spinning nuclear magnetic resonance (NMR)[18,19] (see Box 1); the relative proportions of such tetrahedral configurations have been estimated[18] from the NMR data to be 25% E_0, 50% E_1 and 25% E_2. The corner-sharing bonds associated with such E_0 and E_1 units cause a cross-linking of the chains, and it has been postulated[17] that 'cross-linked chain clusters' are formed—that is, rings containing chain-like fragments consisting of four E_1 and two E_0 units (see Fig. 3). A modelling study[13,14] demonstrated that the neutron diffraction data[11,12] are best fitted by a mixture of structural groupings (Fig. 3), including ~15% of cross-linked chain clusters, with the rest of the structure in the form of random chains of linked tetrahedra, each containing an average of seven E_2 units. In ~15% of these random chains, two chains run locally parallel over a correlation length corresponding to two or three E_2 units. This is perhaps one of the most comprehensive pictures we have yet of the type and extent of MRO in the structure of an inorganic amorphous solid.

The Raman spectra of AX_2-like glasses are generally rich[20], with many narrow lines, surprising in a noncrystalline solid where the effect of structural disorder is generally to broaden Raman lines substantially in comparison with those characteristic of crystals. There are two reasons for this broadening: the absence of periodicity means that, in glasses, extended vibrational excitations ('phonons') cannot be described in terms of k-states, with the consequence that selection rules associated with optical transitions are relaxed and all regions of the vibrational density of states are optically accessible; furthermore, the structural disorder characteristic of noncrystalline materials generally broadens features in the vibrational density of states. Nevertheless, in chalcogenide glasses in general, and AX_2-like materials in particular, vibrational spectra (for example, Raman spectra) have sharp ('molecular-like') peaks as a result of vibrational decoupling[21] of modes associated with cation-centred structural units (such as AX_4-like tetrahedra) because the bridging chalcogen atoms have bond angles near 90°.

One particular narrow peak in the Raman spectrum of AX_2-type glasses has long been associated with MRO because of its anomalously strong dependence[22] on composition: it was

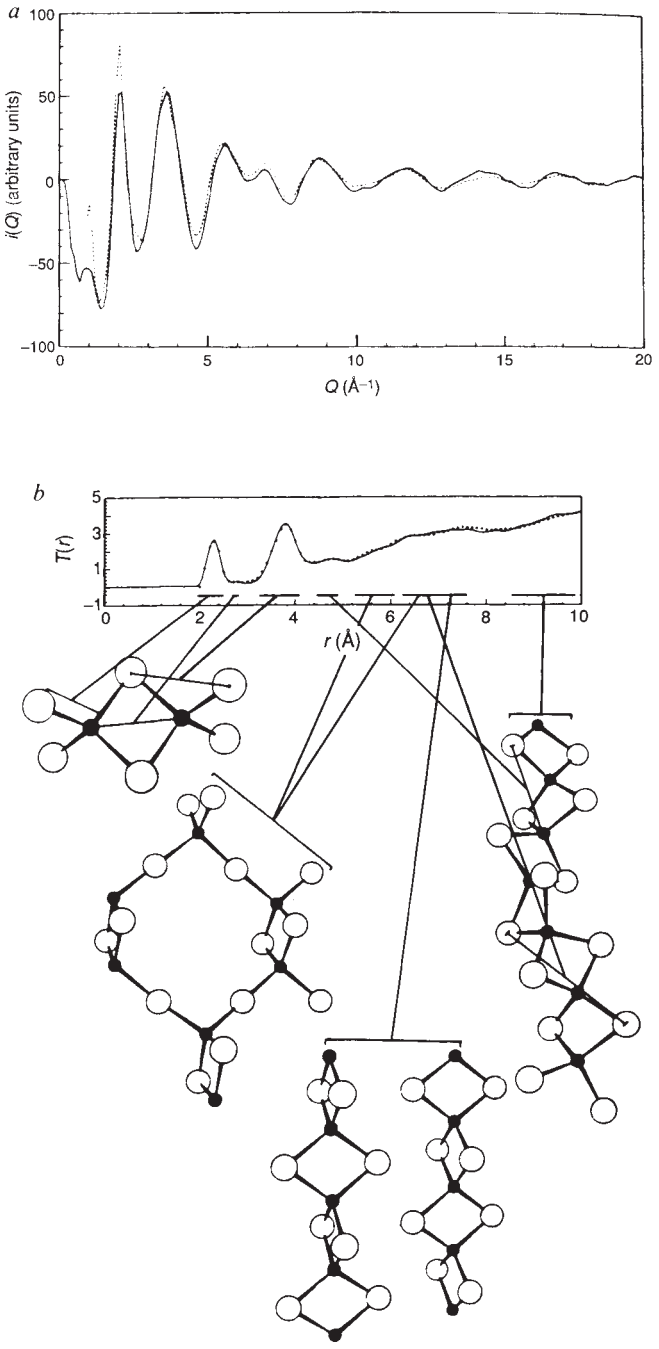

FIG. 3 Experimental neutron diffraction data[11,12] for g-$SiSe_2$ compared with the results of a structural model[13,14]. *a*, Neutron-scattering intensity function (dashed line, experiment; solid line, model). *b*, Radial distribution function (dashed line, experiment; solid line, model). Also shown are the contributions to designated regions of the overall radial distribution function of two-body correlations associated with different structural groupings.

assumed to be a vibrational mode associated with larger-scale structural features, characteristic of MRO, that are broken up preferentially when the composition changes. In the case of g-$GeSe_2$, this anomalous Raman peak occurs as a small, strongly polarized peak at ~220 cm^{-1} (26.5 meV) associated with the prominent A_1 symmetric-stretch 'breathing' mode of $GeSe_4$ tetrahedra which lies at ~200 cm^{-1} (25 meV). It has therefore been termed[23] the 'companion line'. The structural origin of this companion line has long been controversial. Originally, it was ascribed to vibrations of large regular rings[22], and later[23] to the vibrations of wrongly bonded Se-Se 'dimers' postulated to lie at the edges of 'rafts', a term referring to layer-like moieties of the crystalline structure (see Fig. 2*a*). Such rafts are too ordered, however, to be consistent with the diffraction data for the glass[8]. The present consensus of opinion[20,24] seems to be that the companion Raman line in AX_2-like glasses is simply associated with vibrations of the four-membered (A_2X_2) rings characteristic of edge-shared connections between tetrahedra. Presumably, this type of connection is particularly sensitive to rupture for departures of the composition from the stoichiometric composition AX_2.

Rings

Rings of atoms in a covalently bonded amorphous network only become a feature of MRO if they exist either in a proportion greater than expected for an 'ideal' continuous random network of the material (that is, they are 'superstructural' units) or if they are more regular than would otherwise be expected (that is, there is a pronounced well-defined correlation between neighbouring dihedral angles). I have already mentioned one type of ring structure that is characteristic of MRO, the four-membered A_2X_2 rings associated with edge-sharing tetrahedra in AX_2 glasses. These rings will not be discussed further in this section, however, attention being paid to larger rings.

Perhaps the most celebrated example of a ring acting as a superstructural unit in the structure of a glass is the 'boroxol' ring found in g-B_2O_3. This is a regular, planar, six-membered B_3O_3 ring, composed of three corner-sharing planar BO_3 triangles (the basic structural unit in B_2O_3) joined together in a triangular arrangement through their apices (see Fig. 4*a*). The most striking experimental manifestation of the boroxol ring is in the Raman scattering spectrum (Fig. 4*a*): a highly polarized and very narrow peak is observed at 808 cm^{-1}, indicative of a

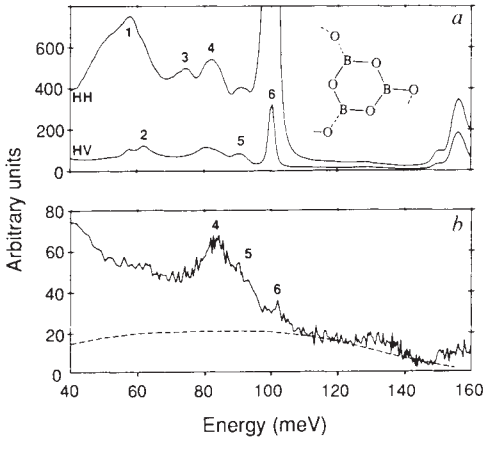

FIG. 4 Vibrational spectroscopy of g-B_2O_3. *a*, Raman spectra[25] showing the highly polarized, narrow band at 100 meV (808 cm^{-1}) ascribed to the symmetric-stretch breathing mode of the oxygen atoms in a boroxol ring (see inset). HV and HH refer to different polarization configurations of the incident and scattered light (H, horizontal; V, vertical). *b*, Inelastic neutron scattering spectrum[29], indicating the absence of a significant feature in the vibrational density of states at 100 meV (808 cm^{-1}).

symmetrical stretching vibrational mode which is localized because of appreciable vibrational decoupling of the mode from other extended (phonon-like) vibrational modes associated with the framework structure. There is no change in the 808-cm^{-1} Raman line on substituting a different B isotope, but there is a pronounced shift in frequency when the O isotope is changed[25]. This implies that only O motion is involved in the vibrational mode responsible for the 808-cm^{-1} Raman peak, and the observed 1:3:3:1 intensity ratio for the resolved quadruplet line when a 50:50 mixture of ^{16}O and ^{18}O isotopes is present is consistent with a random isotopic substitution in a structural unit containing just three O atoms, such as the boroxol ring[25]. It is well known[1] that matrix-element enhancement of symmetric vibrational modes can occur in Raman spectra, making Raman scattering a particularly powerful probe of MRO in the form of regular rings, but it may not be a quantitative probe for structural features that are associated with MRO and are responsible for a particular vibrational mode (see Box 1). This ambiguity has led to considerable controversy[26] over the proportion of boroxol rings in the structure of g-B_2O_3. Estimates for the fraction, f, of B atoms in boroxol rings have been inferred from neutron diffraction data[27] ($f = 0.6$) and from ^{11}B NMR experiments[28] ($f = 0.8$); for comparison, a value of $f = 0.75$ corresponds to a network containing equal numbers of boroxol rings and independent BO_3 triangles. But recent inelastic neutron scattering experiments[29] of g-B_2O_3 (where the coupling constants relating the scattering intensity to the vibrational displacement amplitudes are not enhanced anomalously for the case of symmetric modes) have shown that only a very small peak is seen in the vibrational density of states at 808 cm^{-1}, indicating perhaps that the concentration of boroxol rings in this material is lower than originally believed.

Similar, but less intense, narrow polarized Raman lines have been observed in other oxide glasses. For example in g-SiO_2, two such lines at 495 cm^{-1} (D_1) and 606 cm^{-1} (D_2) are clearly apparent in the Raman spectrum[30]. The structural origin of these Raman bands has been contentious but, on the basis of isotopic substitution experiments, the D_2 line has been ascribed to the symmetric breathing mode involving O atoms in a planar six-membered (Si_3O_3) ring (topologically similar to the boroxol ring), and the D_1 line has been ascribed more tentatively to the same motion in a regular, but slightly puckered, eight-membered ring. The O motion in such rings is vibrationally decoupled from the rest of the network if the ratio of the bond-bending and bond-stretching force constants satisfies a particular analytical relationship involving the angles subtended within the rings at the Si and O atoms[31]. Actual numerical calculations of the vibrational density of states for a continuous random network (CRN) of g-SiO_2 containing six- and eightfold rings have demonstrated, however, that narrow vibrational bands are only obtained if the rings are extremely regular[32]. The structural origin of these Raman features therefore remains in some doubt.

Other noncrystalline systems where rings are believed to play an important part in the structure are the elemental chalcogens, amorphous sulphur and selenium. In the case of sulphur, for example, the various crystalline polymorphs are composed of packings of discrete cyclo-octasulphur (S_8) rings. On melting, the integrity of the rings is preserved until the well-known λ-transition occurs ($T_\lambda = 433$ K), where the rings rupture to form long polymeric chains, thereby causing the viscosity to increase markedly. There has been a long-standing debate about the structure of sulphur (and selenium) glasses quenched from the melt with respect to the relative proportions of rings and chains. Neutron scattering[33] indicates that the structures of molten sulphur and sulphur glass are similar, and significantly different from the structure of a noncrystalline aggregate of S_8 rings predicted by a molecular-dynamics simulation,[34] indicating that chains are the dominant structural motif. The same situation seems to prevail in g-Se.

Clusters

Well-defined clusters of atoms can be regarded as being orientationally ordered arrangements of regular rings and, as such, they represent the next stage in the hierarchy of MRO. As for the case of rings themselves, clusters may be discrete (that is, unconnected by covalent bonds to the rest of the network), in which case the structure consists of a packing of such clusters, or they may be fully incorporated into the matrix of the glass, thereby contributing local regions of high MRO. Several covalently bonded amorphous solids have cluster-like MRO.

One example is the elemental pnictogen, amorphous red phosphorus, made by heat-treating white phosphorus. This material produces a very pronounced first sharp diffraction peak (see Box 2) in the structure factor[35], often taken to be a signature of appreciable MRO, and the Raman spectrum[36] is remarkably structured for an amorphous solid, the most prominent band at $\sim 350\ cm^{-1}$ being strongly polarized, indicative of a symmetric vibrational mode (see Fig. 5*a*). The Raman spectrum of the monoclinic 'Hittorf' crystalline polymorph of phosphorus is remarkably similar to that observed in the amorphous solid (see Fig. 5*a*), and calculations of the vibrational characteristics of the cage-like P_8 and P_9 clusters found in the Hittorf form demonstrate that symmetric breathing modes of these clusters are responsible for the sharp, polarized features observed in the Raman spectrum of the amorphous material[36]. In the crystalline phase, the P_8 and P_9 clusters are connected together to form extended 'tubes' with a pentagonal cross-section (see inset to Fig. 5*a*). In the amorphous phase, however, it is very unlikely that this type of order persists; it is more probable that isolated P_8 or P_9 clusters occur, embedded in and covalently bonded to a matrix composed of a threefold coordinated continuous random network[37].

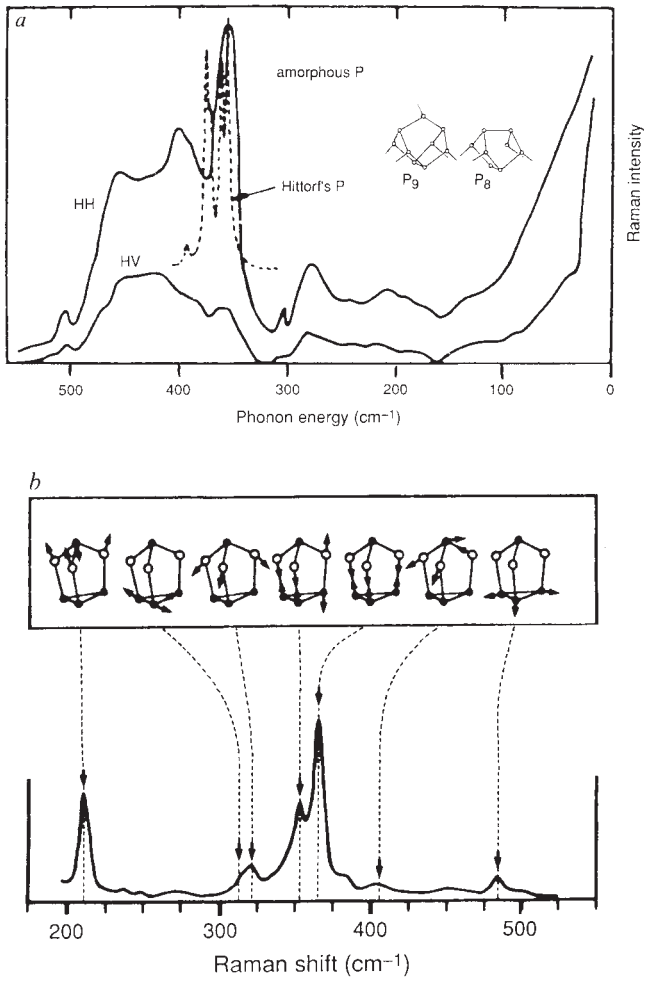

FIG. 5 Cluster-like MRO in amorphous solids. *a*, Raman spectra[36] of a-P, with, inset, the P_8 and P_9 clusters (characteristic of the monoclinic 'Hittorf' crystalline polymorph), the vibrational modes of which are believed to be responsible for the sharp peaks in the spectrum. *b*, Raman spectrum[48] of g-P_2Se. Peaks are assigned in terms of the vibrational modes of a P_4Se_3 molecule (inset).

Discrete cluster-like molecular species have been identified in some amorphous chalcogenide systems. In the case of as-deposited, evaporated amorphous thin films of arsenic sulphide, diffraction data can be interpreted satisfactorily in terms of a packing of almost spherical As_4S_4 molecules (weakly bonded together by van der Waals interactions), with minimal cross-linking between (ruptured) molecular species[38,39]. Such a structure is, perhaps, not too surprising, as the stable vapour species above a melt of As_2S_3 are As_4S_4 and S_2 molecules.

Perhaps the most interesting of all amorphous chalcogenide materials in relation to MRO is the P-Se system, because of its propensity to form P_4Se_n ($n = 3$–10) cage-like molecular clusters[40]. In Se-rich P-Se glasses, neutron diffraction and extended X-ray absorption fine structure measurements[40], as well as magic-angle spinning NMR spectra[19,41], provide evidence for some P_4Se_n clusters (mainly with $n = 10$ for high Se contents) embedded in an amorphous Se matrix. The P_4Se_{10} molecule has four terminator P=Se double bonds oriented in a tetrahedral manner; in the melt-quenched glass, it is probable that these double bonds break, with the result that the four terminating Se atoms can form covalent cross-links to the rest of the structure. Recent ^{31}P spin-echo and magic-angle NMR experiments[42] on Se-rich P-Se glasses, however, indicate that clustering may be less prevalent than previously believed.

The more interesting glass is P_2Se, which has also been studied using neutron diffraction[44,45], extended X-ray absorption fine structure[46] and NMR[41,43]. Here, there is overwhelming evidence that the structure consists almost entirely of discrete quasi-spherical P_4Se_3 cage-like molecules (see inset to Fig. 5*b*), with a small excess of P. For example, the neutron static structure factor, $S(Q)$ (see Box 2) for g-P_2Se can be fitted almost exactly for $Q \geq 6\ Å^{-1}$ by the form factor calculated for the P_4Se_3 molecule[44,45]. Inelastic neutron scattering measurements[47] reveal a highly structured vibrational density of states, the peaks in which can be assigned to the vibrational excitations of a P_4Se_3 molecule. Raman spectra[48] support this assignment, and the higher resolution of Raman scattering compared with inelastic neutron scattering allows more of the vibrational modes to be distinguished (Fig. 5*b*). Finally, quasi-elastic neutron scattering measurements[45] of g-P_2Se have revealed a quasi-elastic broadening of the elastic line at elevated temperatures (300–400 K) (but below the glass-transition temperature, $T_g = 438$ K), indicating the presence of (diffusive) atomic motion. These observations have been interpreted[45] in terms of a rotational diffusional motion of discrete P_4Se_3 molecules (whose centres of mass are randomly distributed in the glassy structure), similar to that which occurs in the plastic phase ($T \geq 355$ K) of crystalline P_4Se_3. Measurements from ^{31}P spin-echo NMR[43] have also provided evidence for orientational mobility of these units. Thus, g-P_2Se may be the first known example of an inorganic 'plastic glass', where topological and dynamic orientational disorder are present simultaneously.

Future prospects

Much progress has been made recently in our understanding of medium-range order in the structure of glasses, particularly of covalently bonded materials where 'superstructural units' (such as regular rings or clusters) are prevalent. But much remains unclear and ill-understood. It seems that further substantial progress in this area will only come from additional advances in experimental techniques and in theoretical descriptions of the disordered state of matter.

On the experimental side, it is very desirable that new techniques are developed which are more sensitive to conformation

(or orientational order) in disordered materials. One potentially powerful method involves NMR, in which conformational and connectivity information can in principle be obtained from interactions such as J–J couplings in two-dimensional spectra[49]. Although this approach has often been used to study conformations of organic molecules in the liquid state, typically using two-dimensional homonuclear shift-correlated spectroscopy (COSY), its use in solid-state studies is hampered by the line-broadening interactions (such as dipolar, quadrupolar or chemical-shift anisotropic) which are normally dominant in solids. Nevertheless, line-narrowing techniques, such as magic-angle spinning and certain multiple-pulse sequences, can be used in such cases, and it is conceivable that under favourable circumstances, conformations (of, for instance, rings, chains or clusters) and connectivities of atoms in amorphous solids could be investigated in this way. Recently, ^{29}Si magic-angle spinning NMR COSY experiments have been used on glasses to investigate the connectivity of Si sites in silicates[49]. Phosphorus-containing glassy solids (such as phosphates or phosphorus chalcogenides) may also be amenable to this approach.

It has been suggested[50] that nonlinear optics could be an experimental probe for local chiral ordering in amorphous covalent solids. For amorphous tetrahedrally coordinated materials (Si, Ge), chirality has been discussed in terms of the dihedral angle, ϕ, associated with six-membered rings in the structure[50,51]. Perfect 'boat-like' ($\phi = 0°$) and 'chair-like' ($\phi = 60°$) rings both have mirror symmetries, whereas the 'twisted-boat' ring ($\phi \neq 0°, 60°$) has only 2-fold rotation symmetry and no mirror symmetry: twisted rings therefore occur in enantiomorphous pairs, each with a distinguishable 'left-hand' ($-60° < \phi < 0°$) and 'right-hand' ($0° < \phi < 60°$) chirality[50]. Although amorphous materials must be (optically) isotropic overall on a macroscopic scale, in principle domains of different chirality could exist on an intermediate microscopic scale. Examination[51] of an all-even-ring model[52] of a-Si(Ge) has demonstrated that it contains rings mostly of the same handedness. Incoherent three-wave mixing (second-harmonic generation) has been suggested[50] as an experimental probe of such local chirality, at least in the 'inverse electro-optic' limit where two incident waves, having nearly the same (high) frequency, are mixed, and the response at a (low) difference frequency is monitored. Here, the intensity of the scattered radiation should be a direct measure of the size of the chiral coherence lengths. Such experiments have not yet been done on covalent amorphous solids, but it is more likely that chirality would be measurable in this way for stoichiometric chalcogenide or oxide glasses

BOX 2 The first sharp diffraction peak

A feature of diffraction data of covalently bonded amorphous solids which has long been associated with the presence of MRO is the 'first sharp diffraction peak' (FSDP) occurring at values of scattering vector Q = 1–2 Å^{-1}, depending on the material. The structural origin of the FSDP has, however, been extremely controversial.

The FSDP is anomalous in a number of ways. It is considerably narrower than the other peaks in the structure factor, $S(Q)$—hence its name. Furthermore, its behaviour as a function of temperature and pressure differs from that of the other peaks in $S(Q)$: in chalcogenide glasses, the FSDP increases (reversibly) in intensity with increasing temperature[67], whereas other peaks in the structure factor decrease in intensity with increasing temperature according to the normal Debye–Waller behaviour; with increasing pressure, it rapidly decreases in intensity, and shifts to higher Q (refs 68, 69), unlike other peaks in $S(Q)$.

Detailed microscopic understanding of the structural origin of the FSDP has remained elusive[1]. For the case of AX_2-type chalcogenide glasses (where A is Si, Ge; X is O, S, Se, Te), however, it seems that cation-centred correlations (A–A and, to a lesser extent, A–X) are primarily responsible for the FSDP. Such evidence has come from anomalous X-ray scattering experiments[70] on g-$GeSe_2$, from isotopic substitution neutron diffraction experiments on (liquid) $GeSe_2$ (ref. 71) and from molecular-dynamics simulations[10] of the structure of g-$GeSe_2$. Finally, although the FSDPs of different chalcogenide and oxide glasses are seen at different scattering vectors, Q_1, when the structure factors are scaled to the nearest-neighbour bond-length, r_1, the FSDPs appear rather similar (ref. 72; see Fig. 6).

Proposals made in the past for the MRO structural origin of the FSDP can be divided into two categories: quasi-crystalline structural configurations or clusters.

Because the crystal structures of many glass-forming chalcogenides (for example, As_2S_3 or $GeSe_2$) are layer-like, it was natural to identify the FSDP with a Bragg-like peak in the scattering factor. For example, the (020) Bragg peak of the orpiment crystalline polymorph of A_2S_3 occurs at a very similar Q to that at which the FSDP is observed in the glassy phase[73]. Thus, it has been assumed that pseudo-crystalline layer-like structural arrangements with spatial repeat d are present in the glass[67]; the FSDP position is then given roughly by $Q_1 \approx 2\pi/d$. This pseudo-crystalline model is inconsistent, however, with some experimental observations. The FSDP is also produced by some chalcogenide materials in the liquid state[74]; it is extremely unlikely that pseudo-crystalline arrangements having correlation lengths 20–30 Å should survive in the liquid. Furthermore, and perhaps more tellingly, a layer-like interpretation cannot be a general explanation for the occurrence of the FSDP, as the feature is observed even in glasses (such as SiO_2), where the crystalline polymorphs are not layer-like. Nevertheless, the attraction of an interpretation in terms of parallel ordered configurations remains strong; recent work[75] has shown that structural correlations between pairs of ribbon-like structural configurations in GeS_2 or $GeSe_2$ can in certain circumstances give rise to a FSDP[75].

Another explanation for the FSDP involves correlations between (ill-defined) clusters. It is well known[76] that the structure factors of molecular liquids, such as CCl_4, also show sharp, well-defined FSDPs (albeit at different values of Q from those characteristic of inorganic glasses). For such systems, $S(Q)$ can be regarded as the sum of two distinct terms, one arising from intermolecular correlations and given by an intermolecular interference function, $D_m(Q)$, and the other resulting from intramolecular correlations and given by a molecular form factor $f_m(Q)$: that is, $S(Q) = D_m(Q) + f_m(Q)$. Because intramolecular correlations in molecular liquids are well defined, the oscillations in $f_m(Q)$ persist to high values of Q and are the dominant contribution to $S(Q)$ in this region. Intermolecular correlations are much less well defined, and consequently peaks in $D_m(Q)$ are rapidly damped with increasing Q. Either the first, and most prominent, peak in $D_m(Q)$ forms the first peak in $S(Q)$, in other words the FSDP, or else it is an artefact resulting from the addition of a decreasing function ($f_m(Q)$) and an increasing function ($D_m(Q)$). In this picture, the FSDP by itself therefore has minimal structural significance. The role of correlations between clusters in producing the FSDP in chalcogenide, oxide and other glasses has also been stressed[77,78]; in general, however, the structural identity of such clusters in glasses remains obscure.

I have recently proposed a new explanation[79], in which the FSDP is ascribed to a chemical-order pre-peak (in the concentration–concentration partial structure factor, $S_{cc}(Q)$, in the Bhatia–Thornton formalism[80]), arising from the clustering of interstitial voids around cation-centred 'clusters'; in the case of AX_2-type glasses, the clusters are taken to be the AX_4 tetrahedra themselves. Blétry[81] has discussed the structure of the tetrahedrally coordinated elemental amorphous semiconductors, a-Si and Ge, in terms of a packing of atoms and atom-sized voids, and he ascribed the first peak in $S(Q)$ at $Q \approx 2$ Å^{-1} (not previously regarded as an FSDP in these cases) to a pre-peak in $S_{cc}(Q)$ resulting from the chemical ordering voids around the atoms. I believe, however, that clustering of smaller interstitial voids around clusters of atoms in covalently bonded glasses (and liquids) is a general occurrence, and this feature is the reason for the ubiquity of the FSDP in these materials. A recent interstitial-void analysis of models of v-SiO_2, for example, has shown that such voids are situated at remarkably well-defined distances from Si (but not O) atoms[82].

This association of the FSDP with correlations involving interstitial voids naturally explains the observed effect of pressure: the application of pressure causes a densification of the glass structure through a diminution of interstitial volume, thereby leading to a decrease in the intensity of the FSDP. The anomalous temperature dependence of the FSDP essentially occurs because, as the temperature of a glass increases, its density decreases. The survival of the FSDP into the molten state can also naturally be understood on this basis.

(such as AX_2 or B_2X_3 systems), where all rings are even (recall, for instance, that the crystalline polymorph of silica, quartz, is chiral), than for the amorphous elements, Ge or Si, where the structure is likely to be a mixture of even and odd rings with negligible net chirality[51].

Nevertheless, optical activity can, under certain circumstances, probe chirality in glasses[50]. In recent experiments on bulk glassy semiconducting As_2S_3, both natural and photo-induced optical activities were observed[53]. Moreover, considerable diffuse light scattering was observed after optical excitation of the glass[53]; this behaviour could result from optically-induced changes in local optical activity[50]. Possible local chiral units in the structure of As_2S_3 are helical chains of As and S atoms (cross-linked at the As atoms by bridging S atoms). These are present in the crystal structure, and models[54] indicate that they are present, to a lesser degree, in the structure of glassy As_2S_3. Although the origin of optically induced optical anisotropy in chalcogenide glasses is not yet understood, it is conceivable that the absorption of polarized light by glassy As_2S_3 causes a 'flipping' of twofold coordinated S atoms in helical sites so that a degree of local helical order is established—that is, domains of local chirality are produced. The possible use of photo-induced optical anisotropy in chalcogenide glasses as a probe of local chirality warrants further study.

There are many gaps in our theoretical understanding of medium-range order in the structure of glasses. Here I have adopted the (geometric) approach that MRO can be regarded as being related in an hierarchical way to short-range order in the case of covalently bonded amorphous materials. This has been termed 'propagated' SRO elsewhere[55]. The viewpoint is useful because, in such materials, the SRO is so well defined, with such strong orientational directionality, that correlations in position and orientation between neighbouring structural units are very likely.

In certain cases, however, the converse may be true: stereochemical SRO may be a consequence of the existence of a well-defined MRO[56]. This idea has been proposed[56,57] specifically for the case of transition metal–metalloid (TMM) glasses, such as $Pd_{80}Si_{20}$. In the case of crystalline TMM materials, trigonal prismatic coordination of metalloid atoms can be regarded as arising from the introduction of 'chemical twinning' planes containing the metalloid atoms into close-packed crystalline arrangements of the metal atoms; the composition of the TMM alloy can be varied by changing the periodicity of the chemical twinning planes. In glasses of these materials, it has been suggested[57] that MRO is associated with domains of size 10–20 Å, within each of which there are more-or-less ordered arrays of chemical twinning planes, and in such planes are therefore located the trigonal prismatic units which are believed to characterize the SRO in these amorphous metals; the assumption is that disorder is introduced by the orientation of the twinning planes being different in each domain.

The MRO may also determine the SRO in other (pseudo-) close-packed noncrystalline systems. One example concerns alkali or alkaline earth silicate glasses[56], where the O anions can be regarded as being effectively nearly close-packed, and (some of) the interstices can be regarded, to a first approximation, as the sites occupied by the alkali or alkaline-earth 'modifier' cations.

A second-difference, isotope-substitution neutron diffraction study of a calcium silicate glass[58], providing direct evidence for Ca–Ca correlations, has revealed that the Ca ions are not distributed randomly in the silicate matrix, but instead seem to occupy octahedral interstices in the O sublattice (as in the corresponding crystal). Furthermore, these CaO_6 octahedra seem to be connected by edge-shared connections, resulting in sheet-like structures (again as found in the corresponding crystal), and these layers are interconnected by SiO_4 tetrahedra, the Si atoms therefore occupying the tetrahedral interstices in the O packing. Thus, the SRO of the Ca^{2+} cations can be regarded as resulting from the MRO associated with the close-packed O sublattice.

For alkali silicate glasses, the picture seems to be similar. Magic-angle spinning NMR has revealed that, at certain stoichiometric compositions, essentially only one type of SiO_4 tetrahedral species exists, as described by the number n, of bridging oxygens per tetrahedron (denoted Q_n, $n = 0$–4). For the case of disilicate glass compositions, for example, Q_3 species are dominant[59]: that is, there is only one negatively charged non-bridging O atom per SiO_4 tetrahedron, as in the corresponding crystal. In reality, however, there is some speciation even at stoichiometric compositions, most notably in the lithium silicates[59]. The observation of preferred Q_n species at certain compositions, instead of a statistical distribution determined by the composition, implies, of course, that the local structural environment (SRO) of the alkali modifier cations is also highly ordered.

A recent attempt[60] to understand the variation with composition of the proportion of different Q_n species in alkali silicate glasses uses a thermodynamic approach involving disproportionation equilibria between the species; this approach would be valid in the molten state, and the resulting distributions of Q_n species are assumed to be frozen in on quenching the melt through the glass-transition temperature to form the glass. It was found that the quantity that determines the distribution is the 'bond-ordering energy' arising from the (coulombic) interaction between non-bridging and bridging O sites, $\Delta E = E_{BB} + E_{NN} - 2E_{NB}$ (where B and N refer to bridging and non-bridging oxygens respectively), rather than the configurational entropy. Thus, the structure of alkali silicate glasses would be

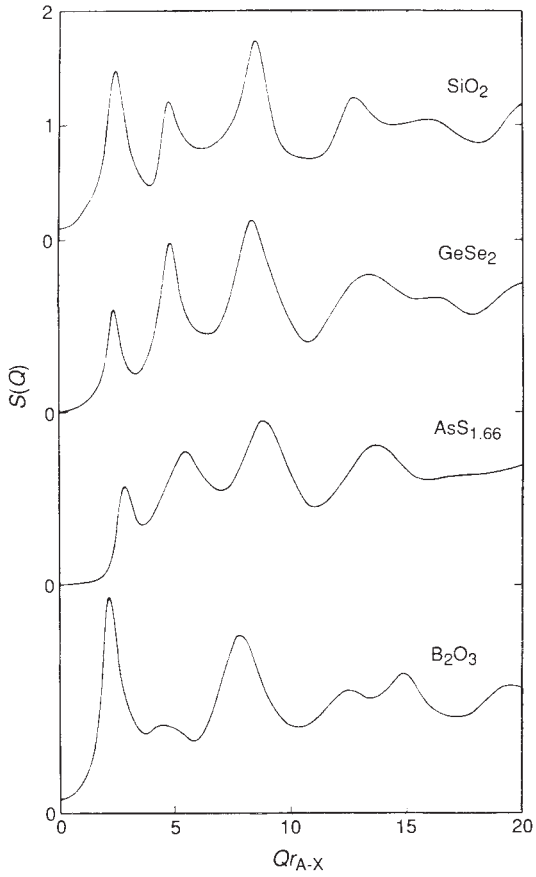

FIG. 6 Structure factor, $S(Q)$, for some oxide and chalcogenide glasses plotted[72] against the reduced variable Qr_1, where r_1 is the nearest neighbour bond length in each case, showing the roughly constant position of the FSDP in this representation.

controlled by the need to minimize the coulombic repulsion between non-bridging oxygens. This condition determines the distribution of Q_n species, in turn determining the local (SRO) environment of the alkali cations which, in this sense, do not 'modify' the structure at all, their sole effect being to determine the overall number of non-bridging O sites by charge balance.

From a theoretical point of view, computer simulations of structures of amorphous solids should provide considerable insight into the nature and origin of MRO. Progress has recently been made in molecular dynamics simulations by the inclusion of empirical three-body interaction terms in the potential-energy expressions, to try to mimic the effect of non-centrosymmetric (covalent) forces on the structure; this approach has been used, for example, for v-SiO_2 (refs 61, 62) and v-$GeSe_2$ (ref. 10). A more powerful approach is to use potentials that are derived quantum-mechanically in a self-consistent way using first-principles methods, as in the pioneering work of Car and Parrinello (ref. 63); this approach suffers at present, however, from limitations in computing power, which restrict the number of atoms that can be treated. A further limitation of molecular dynamics for simulating glassy structures is that the simulated cooling rates from the liquid state are many orders of magnitude higher than those encountered experimentally. As a result, one must question whether details of subtle structural features, such as those involving MRO, in models resulting from such simulations are truly representative of real glassy materials. But molecular dynamics simulations have the undoubted advantage that, uniquely, they span the transition from liquid to glassy solid and so can be used to ascertain the effect of different types of MRO on the temperature-dependent viscosity behaviour of different systems, and hence ultimately on the glass-forming propensity of liquids.

Finally, a more abstract way of regarding the structure of noncrystalline materials is as a projection, onto normal three-dimensional euclidean space, of geometric entities ('polytopes') which are regular in a curved, non-euclidean space of higher dimensionality (for a review of this approach, see ref. 64). A formal analogy exists between this approach and that employed to understand the structure of quasi-crystals: in the latter, three-dimensional Penrose tilings—an aperiodic model for the structure—can be generated as a projection from a six-dimensional hypercubic lattice on a three-dimensional hyperplane lying at an incommensurate orientation (see refs 65, 66). In certain cases, symmetries of the polytope will be approximately preserved locally on mapping. For example, rotational symmetries of the polytope in curved space appear as approximate translational symmetries in euclidean space[55]. An intriguing consequence of the existence of regions of such 'polytope-like' order in the structure of real amorphous solids would be that for these domains, an approximately vertical selection rule governing optical absorption should exist[55], as in crystals: $(k_f - k_i) \approx 0$ (where k_f and k_i are the electron wavevectors corresponding to the final and initial states, respectively). Generally, for noncrystalline materials no such selection rule exists, as the electron wavevector is ill defined in the absence of translational periodicity[1]. Sharp features in the optical (vibrational) spectra of glasses (see, for example, Figs 4 and 5), conventionally regarded as indicating MRO in the form of clusters or rings when vibrational decoupling between modes occurs, could possibly be interpreted instead as a result of polytope-like order. It is interesting to speculate, therefore, to what extent pronounced features of MRO in the structure of real amorphous solids (such as clusters) could be a signature of order in a higher dimensional representation of the disordered structure. □

S. R. Elliott is in the Department of Chemistry, University of Cambridge, Lensfield Road, Cambridge CB2 1EK, UK.

1. Elliott, S. R. *Physics of Amorphous Materials*, 2nd Edn (Longman, London, 1990).
2. Boolchand, P. in *Physical Properties of Amorphous Materials* (eds Adler, D., Schwartz, B. B. & Steele, M. C. 221–260 (Plenum, New York, 1985).
3. Lucovsky, G. *J. non-cryst. Solids* **97–98,** 155–158 (1987).
4. Cervinka, L. *J. non-cryst. Solids* **97–98,** 207–212 (1987).
5. Galeener, F. L. in *The Physics and Technology of Amorphous SiO_2* (ed. Devine, R. A. B.) 1–13 (Plenum, New York, 1988).
6. Zallen, R. *The Physics of Amorphous Solids* (Wiley, New York, 1983).
7. Phillips, J. C. *J. non-cryst. Solids* **43,** 37–77 (1981).
8. Wright, A. C., Price, D. L., Clare, A. G., Etherington, G. & Sinclair, R. N. *Diffusion Defect Data* **53–54,** 255–263 (1987).
9. Susman, S., Volin, K. J., Montague, D. G. & Price, D. L. *J. non-cryst. Solids* **125,** 168–180 (1990).
10. Vashishta, P., Kalia, R. K., Antonio, G. A. & Ebbsjö, I. *Phys. Rev. Lett.* **62,** 1651–1654 (1989).
11. Johnson, R. W. *et al. J. non-cryst. Solids* **83,** 251–271 (1986).
12. Johnson, R. W. *J. non-cryst. Solids* **88,** 366–380 (1986).
13. Gladden, L. F. & Elliott, S. R. *J. non-cryst. Solids* **109,** 211–222 (1989).
14. Gladden, L. F. & Elliott, S. R. *J. non-Cryst. Solids* **109,** 223–236 (1989).
15. Tenhover, M., Hazle, M. A. & Grasselli, R. K. *Phys. Rev. Lett.* **51,** 404–406 (1983).
16. Tenhover, M., Hazle, M. A., Grasselli, R. K. & Thompson, C. W. *Phys. Rev.* B**28,** 4608–4614 (1983).
17. Griffiths, J. E., Malyj, M., Espinosa, G. P. & Remeika, J. P. *Phys. Rev.* B**30,** 6978–6990 (1984).
18. Tenhover, M., Boyer, R. D., Henderson, R. S., Hammond, T. E. & Shreve, G. A. *Solid State Commun.* **65,** 1517–1521 (1988).
19. Eckert, H. *Angew. Chem. Int. Ed. Engl. Adv. Mater.* **28,** 1723–1732 (1989).
20. Sugai, S. *Phys. Rev.* B**35,** 1345–1361 (1987).
21. Sen, P. N. & Thorpe, M. F. *Phys. Rev.* B**15,** 4030–4038 (1977).
22. Nemanich, R. J., Solin, S. A. & Lucovsky, G. *Solid State Commun.* **21,** 273–276 (1977).
23. Bridenbaugh, P. M., Espinosa, G. P., Griffiths, J. E., Phillips, J. C. & Remeika, J. P. *Phys. Rev.* B**20,** 4140–4144 (1979).
24. Nemanich, R. J. *et al. Physica* B**117–118,** 959–961 (1983).
25. Windisch, C. F. & Risen, W. M. *J. non-cryst. Solids* **48,** 307–323 (1982).
26. Williams, S. J. & Elliott, S. R. *Proc. R. Soc. Lond.* A**380,** 427–445 (1982).
27. Johnson, P. A. V., Wright, A. C. & Sinclair, R. N. *J. non-cryst. Solids* **50,** 281–311 (1982).
28. Jellison, G. E., Panek, L. W., Bray, P. J. & Rouse, G. B. *J. chem. Phys.* **66,** 802–812 (1977).
29. Hannon, A. C., Sinclair, R. N., Blackman, J. A., Wright, A. C. & Galeener, F. L. *J. non-cryst. Solids* **106,** 116–119 (1988).
30. Galeener, F. L. *Solid State Commun.* **44,** 1037–1040 (1982).
31. Galeener, F. L., Barrio, R. A., Marinez, E. & Elliott, R. J. *Phys. Rev. Lett.* **53,** 2429–2432 (1984).
32. de Leeuw, S. W., He, H. & Thorpe, M. F. *Solid State Commun.* **56,** 343–346 (1985).
33. Winter, R. *et al. Europhys. Lett.* **11,** 225–228 (1990).
34. Stillinger, F. H., Weber, T. A. & LaViolette, R. A. *J. chem. Phys.* **85,** 6460–6469 (1986).
35. Elliott, S. R., Dore, J. C. & Marseglia, E. *J. Phys.* C8–46, 349–353 (1985).
36. Fasol, G., Cardona, M., Hönle, W. & von Schnering, H. G. *Solid State Commun.* **52,** 307–310 (1984).
37. Greaves, G. N., Elliott, S. R. & Davis, E. A. *Adv. Phys.* **28,** 49–141 (1979).
38. Daniel, M. F., Leadbetter, A. J., Wright, A. C. & Sinclair, R. N. *J. non-cryst. Solids* **32,** 271–293 (1979).
39. Wright, A. C., Leadbetter, A. J. & Sinclair, R. N. *J. non-cryst. Solids* **71,** 295–302 (1985).
40. Price, D. L. *et al. J. non-cryst. Solids* **66,** 443–465 (1984).
41. Lathrop, D. & Eckert, H. *J. non-cryst. Solids* **106,** 417–420 (1988).
42. Lathrop, D. & Eckert, H. *J. phys. Chem.* **93,** 7895–7902 (1989).
43. Lathrop, D. & Eckert, H. *Phys. Rev.* B**43,** 7279–7287 (1991).
44. Verrall, D. J., Gladden, L. F. & Elliott, S. R. *J. non-cryst. Solids* **106,** 47–49 (1988).
45. Verrall, D. J. & Elliott, S. R. *J. non-cryst. Solids* **114,** 34–36 (1989).
46. Verrall, D. J. & Elliott, S. R. in *Neutron and X-ray Scattering: Complementary Techniques* (eds Fairbanks, M. C., North, A. N. & Newport, R. J.) 87–95 (Institute of Physics, Bristol, 1990).
47. Verrall, D. J. & Elliott, S. R. *Phys. Rev. Lett.* **61,** 974–977 (1988).
48. Phillips, R. T., Wolverson, D., Burdis, M. S. & Fang, Y. *Phys. Rev. Lett.* **63,** 2574–2577 (1989).
49. Knight, C. T. G., Kirkpatrick, R. J. & Oldfield, E. *J. non-cryst. Solids* **116,** 140–144 (1990).
50. Di Vincenzo, D. P. *Phys. Rev.* B**37,** 1245–1261 (1988).
51. Di Vincenzo, D. P. & Brodsky, M. H. *J. non-cryst. Solids* **77–78,** 241–244 (1985).
52. Connell, G. A. N. & Temkin, R. J. *Phys. Rev.* B**9,** 5323–5326 (1974).
53. Lyubin, V. M. & Tikhomirov, V. K. *JETP Lett.* **51,** 518–520 (1990); **52,** 722–725 (1990); *J. non-cryst. Solids* **114,** 133–135 (1989).
54. Pfeiffer, G., Brabec, C. J., Jefferys, S. R. & Paesler, M. A. *Phys. Rev.* B**39,** 12861–12871 (1989).
55. Mosseri, R., di Vincenzo, D. P., Sadoc, J. F. & Brodsky, M. H. *Phys. Rev.* B**32,** 3974–4000 (1985).
56. Gaskell, P. H. *Key Engng Mater.* **13–15,** 71–84 (1987).
57. Dubois, J. M., Gaskell, P. H. & Le Caer, G. *Proc. R. Soc. Lond.* A**402,** 323–357 (1985).
58. Gaskell, P. H., Eckersley, M. C., Barnes, A. C. & Chieux, P. *Nature* **350,** 675–677 (1991).
59. Stebbins, J. F. *Nature* **330,** 465–467 (1987).
60. Gurman, S. J. *J. non-cryst. Solids* **125,** 151–160 (1990).
61. Feuston, B. P. & Garofalini, S. H. *J. chem. Phys.* **89,** 5818–5824 (1988).
62. Vashishta, P., Kalia, R. K., Rino, J. P. & Ebbsjö, I. *Phys. Rev.* B**41,** 12197–12209 (1990).
63. Car, R. & Parrinello, M. *Phys. Rev. Lett.* **55,** 2471–2474 (1985).
64. Sadoc, J. F. & Rivier, N. *Phil. Mag.* B**55,** 537–573 (1987).
65. Duneau, M. & Katz, A. *Phys. Rev. Lett.* **54,** 2688–2691 (1985).
66. Elser, V. *Phys. Rev.* B**32,** 4892–4898 (1985).
67. Busse, L. E. *Phys. Rev.* B**29,** 3639–3651 (1984).
68. Tsutsu, H., Tamura, K. & Endo, H. *Solid State Commun.* **52,** 877–879 (1984).
69. Tanaka, K. *Phil. Mag. Lett.* **57,** 183–187 (1988).
70. Fuoss, P. H., Eisenberger, P., Warburton, W. K. & Bienenstock, A. *Phys. Rev. Lett.* **46,** 1537–1540 (1981).
71. Penfold, I. T. & Salmon, P. S. *Phys. Rev. Lett.* **67,** 97–100 (1991).
72. Wright, A. C., Sinclair, R. N. & Leadbetter, A. J. *J. non-cryst. Solids* **71,** 295–302 (1985).
73. Leadbetter, A. J. & Apling, A. J. *J. non-cryst. Solids* **15,** 250–268 (1974).
74. Susman, S., Price, D. L., Volin, K. J., Dejus, R. J. & Montague, D. G. *J. non-cryst. Solids* **106,** 26–29 (1988).
75. Cervinka, L. *J. non-cryst. Solids* **106,** 291–300 (1988).
76. Misawa, M. *J. chem. Phys.* **93,** 6774–6778 (1990).
77. Moss, S. C. & Price, D. L. in *Physics of Disordered Materials* (eds Adler, D., Fritzsche, H. & Ovshinsky, S. R.) 77–95 (Plenum, New York, 1985).
78. Price, D. L., Moss, S. C., Reijers, R., Saboungi, M. L. & Susman, S. *J. Phys.* C**21,** L1069–1072 (1988).
79. Elliott, S. R. *Phys. Rev. Lett.* **67,** 711–714 (1991).
80. Bhatia, A. B. & Thornton, D. E. *Phys. Rev.* B**2,** 3004–3012 (1970).
81. Blétry, J. *Phil. Mag.* B**62,** 469–508 (1990).
82. Chan, S. L. & Elliott, S. R. *Phys. Rev.* B**43,** 4423–4432 (1991).